Electron Compton defect observed in He, H_2, D_2, N_2, and Ne profiles

W. H. E. Rueckner, A. D. Barlas, and H. F. Wellenstein
Department of Physics, Brandeis University, Waltham, Massachusetts 02154
(Received 27 February 1978)

A high-energy electron-impact spectroscopy (HEEIS) apparatus has been constructed for high-precision Compton-scattering experiments. Electron-Compton-scattering experiments are performed by crossing a beam of high energy, but nonrelativistic, electrons with a beam of atoms or molecules and measuring the energy-loss spectrum of the scattered electrons over a range of scattering angles. The improvements of design and technique, the method of data analysis, and the theory used to convert cross sections to Compton profiles are discussed fully. It was found that the energy-loss spectra taken over a range of scattering angles do not reduce by means of the binary-encounter approximation (impulse approximation) to Compton profiles in agreement with theory. This disagreement is most apparent in a shift of the experimental Compton peak—the Compton defect—from the peak predicted by the binary-encounter theory. The Compton defect has been studied in detail for momentum transfers from 1.5–12 a.u. for both He and H_2. Defect measurements for D_2, N_2, and Ne have also been made and it was found that the N_2 and Ne defects were opposite in direction from the He and H_2 defects. The D_2 defect was identical to that for H_2. The electron Compton defect is discussed in relation to other recent defect measurements using x-ray and $(e,2e)$ techniques as well as recent theoretical results. An evaluation of the theory used to convert cross sections to Compton profiles is presented and, on the basis of the defect measurements, it is suggested that, even when the binary-encounter conditions have been attained at large momentum transfers, the binary-encounter theory breaks down in the high accuracy (1%) limit. An explanation for this breakdown is given and recent theories, which at least qualitatively account for the Compton defect, are discussed.

I. INTRODUCTION

The electron-Compton-scattering experiment (see Figs. 1 and 2) consists basically of an electron beam source, a gas jet target, and an electron energy analyzer. Nonrelativistic high-energy electrons of a fixed energy are scattered from atoms or molecules at a fixed scattering angle and incident electron-beam energy.

Since the 1930s electron Compton scattering has become a technique of vast potential resulting from a combination of experimental and theoretical advances. This resurgence was primarily due to Bonham and co-workers. A major improvement in the electron scattering technique was made by Wellenstein and Bonham[1,2] by obtaining an energy resolution 20 times better than that feasible by photon Compton scattering.

The present high-energy electron impact-spectroscopy (HEEIS) apparatus is similar to the one described by Wellenstein *et al.*,[3] but several significant improvements have been achieved. To test the new design and improvements in technique, the data analysis methods and the theoretical model used to convert cross sections to Compton profiles, a study of helium was initially undertaken. Helium is the simplest atom to be studied with the present apparatus and, with the increasing availability of more accurate wave functions, the experimental results can be compared to the excellent Compton-profile calculations which exist for this element.[4]

In the derivations of the Compton line shape for both photon and electron scattering, certain approximations are made. These approximations have come to be known as the impulse approximation (IA) for the photon case and the binary-encounter (BE) theory for electrons.

In the dynamics of the collision process under consideration, the incident electron carries sufficiently high energy to eject the atomic electron with which it interacts. The basic assumptions used in the BE theory[5,6] are (i) that the incident particle interacts with only one target electron and (ii) the mutual interaction between the atomic electrons and nucleus can be disregarded during the collision. These two assumptions are justified only if the effective interaction between the incident and the (ejected) atomic electron takes place in a region which is small compared to the atomic dimensions or, equivalently, that the scattering interaction takes place in a short period of time relative to the mean orbital period of the atomic or molecular electron. This condition is satisfied if (i) the energy transfer is large compared to the binding energy of the atomic electron and (ii) the momentum transfer is large compared to the relevant momentum of the atomic electron. In these respects, the BE theory is analogous to the IA for photon scattering.

Vriens[5,6] has found good agreement between BE collision theory, Born, and plane-wave Born

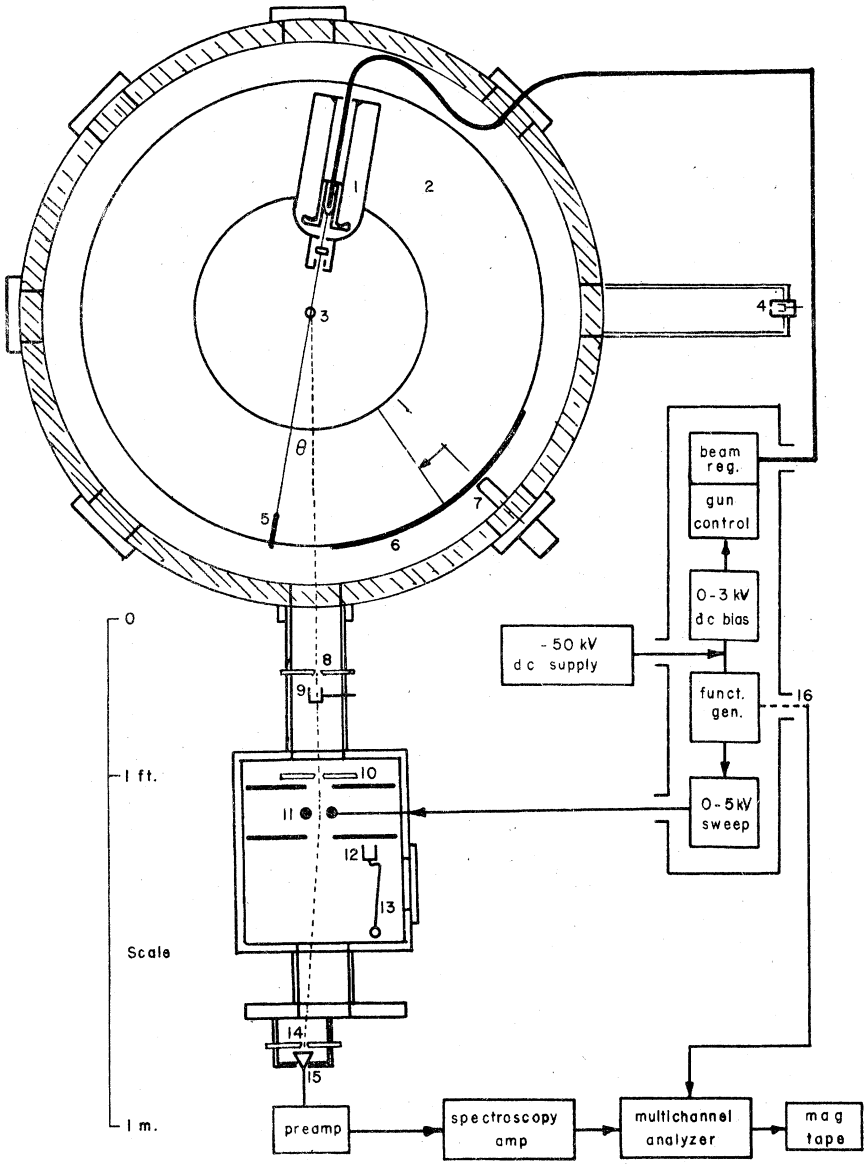

FIG. 1. Schematic diagram of the HEEIS apparatus. Shown are : (1) electron gun, (2) turntable, (3) gas jet, (4) focusing pinhole, (5) beamtrap, (6) angular measurement scale, (7) angular measurement microscope, (8) collimating slits, (9) zero-angle Faraday cup, (10) Möllenstedt slit, (11) high-voltage lens, (12) ghost-electron Faraday cup, (13)fluorescent screen, (14)detector slits, (15) solid-state detector, and (16) light pipe. The general layout of the electronics is also shown.

theory if these conditions are met. This implies that no information about the interaction of the ejected electron with the nucleus or the other atomic electrons is needed to get the correct generalized oscillator strength at large-momentum transfer and incident energy, provided that the correct momentum distribution of the atomic electrons is used.

In this work it was found, however, that the energy-loss spectra do not reduce to Compton profiles when the binary-encounter theory is applied. The discrepancy is most apparent in a shift of the experimental Compton peak, the Compton defect, from the peak predicted by the BE theory. Preliminary Compton-defect results have been published elsewhere.[7] In this work we present extensive results on helium as well as those obtained for molecular hydrogen, molecular deuterium, molecular nitrogen, and neon. A description of the apparatus is given and important experimental parameters affecting the precision of the Compton-defect measurements are discussed in detail. The Compton defect is also analyzed in relation to recent theoretical calculations and results obtained with x rays.

II. THEORY

A. Evaluation of the differential-scattering cross section in the BE approximation

It is assumed that in the limit of high incident energies (as compared to target electron-binding

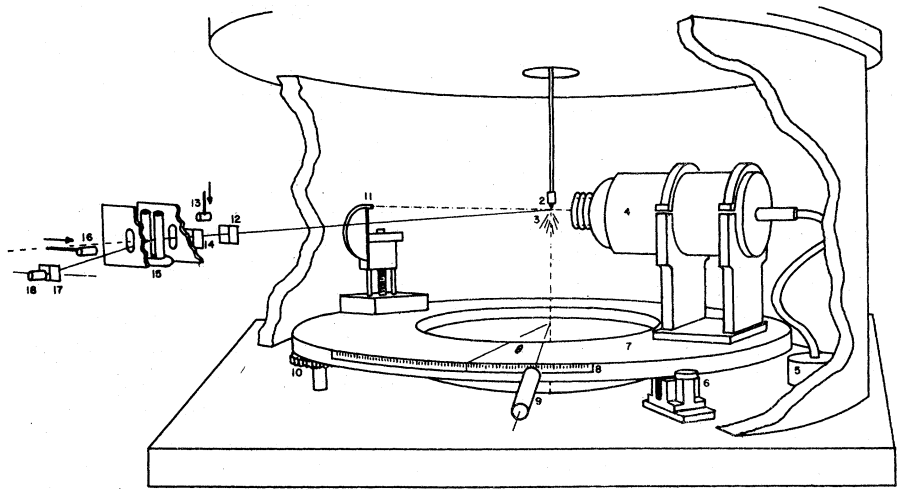

FIG. 2. Cutaway view of the HEEIS apparatus. Shown are: (1) removable vacuum chamber lid, (2) gas-jet nozzle, (3) gas jet, (4) electron gun, (5) HV vacuum feedthrough, (6) turntable bearings, (7) turntable, (8) angular measurement scale, (9) angular measurement microscope (10) turntable drive gear, (11) beamtrap, (12) collimating slits, (13) zero-angle Faraday cup, (14) Möllenstedt slit, (15) high-voltage lens, (16) ghost-electron Faraday cup, (17) detector slits, and (18) solid-state detector. The energy analyzer (1°)–(18) is not to scale with respect to the rest of the apparatus.

energies) that the first Born nonrelativistic theory of scattering is valid. With this assumption and using Fermi's Golden Rule for calculating the transition probability and cross section along the lines of Bethe[8] leads to the differential cross section for direct inelastic scattering cited by Bonham and Tavard[9]

$$\frac{d\sigma}{d\Omega} = \frac{1}{(4\pi)^2} \sum_{n=1}^{M} \left(\frac{k_n}{k}\right) |\langle \psi_n | e^{-i\vec{k}_n\cdot\vec{r}_0} V_e e^{i\vec{k}\cdot\vec{r}_0} | \psi_0 \rangle|^2 , \quad (1)$$

where $\vec{k}$ is the incident wave vector, $\vec{k}_n$ is the scattered wave vector, V is the interaction potential $2(Z/r_0 - \sum_{i=1}^{N} 1/\vec{r}_0 - \vec{r}_1)$ in Rydberg atomic units, with $\vec{r}_0$ the position of the incident electron, and $\vec{r}_1$ the position of the ith of N target electrons for an atom of nuclear charge Z. The sum over n includes all excitations from the target initially in its ground electronic state described by the N-electron stationary-state wave function ψ_0 to the M energetically accessible N-electron stationary target-excited states described by ψ_n. The sum also includes integration over all continuum final states. The matrix elements include integration over all electronic coordinates and summation over all spin coordinates.

The theoretical treatment presented here follows that in Ref. 9. The sum over n which extends over all energetically accessible final states M can be replaced by[10]

$$\sum_{n=0}^{M} = \sum_{n=0}^{\infty} \int_0^{E_0} dE\, \sigma(\epsilon_n - \epsilon_0 - E) ,$$

where ϵ_0 is the total electronic energy of the target ground state, ϵ_n is the total electronic energy of the nth excited target state, E_0 is the incident electron energy, and E is the energy gain suffered by the target on being excited in its nth state. If k_n is regarded as a function of the continuous variable E and use is made of the fact that

$$\sigma(\epsilon_n - \epsilon_0 - E)\,|\psi_n\rangle = \sigma(H - \epsilon_0 - E)\,|\psi_n\rangle ,$$

where H is the target Hamiltonian, closure can be used exactly in Eq. (1) with the result

$$\begin{aligned}\frac{d\sigma}{d\Omega} = \frac{1}{(4\pi)^2} \int_0^{E_0} dE \left(\frac{k(E)}{k}\right) & \\ \times \langle \psi_0 | e^{-i\vec{k}\cdot\vec{r}_0} & \\ \times V(\vec{r}_0) e^{i\vec{k}(E)\cdot\vec{r}_0} \sigma(H - \epsilon_0 - E) & \\ \times (1 - |\psi_0\rangle\langle\psi_0|) e^{-i\vec{k}(E)\cdot\vec{r}_0} V(\vec{r}_0') e^{i\vec{k}\cdot\vec{r}_0} |\psi_0\rangle ,&\end{aligned}$$

where the prime on $\vec{r}_0$ is a reminder that two different integrations over the incident electron coordinate remain to be carried out. The approach used by Bonham and Tavard[9] is to retain the original δ function and develop the entire cross-section expression in the same perturbation expansion. The procedure to be followed is to transform the target wave functions to momentum space and operate on the resulting plane-wave real-space dependence by the energy-conserving δ function by permuting it to the left-hand side, where it can be expanded in powers of suitable terms; the matrix elements are then evaluated term by term. The nuclear terms vanish in first order leaving, after some algebra, the final result

$$\frac{d\sigma}{d\Omega} = 4\int_0^{E_0} \frac{dE\,k(E)}{k[K(E)]^4}\left(\int d\vec{p}\,\rho(\vec{p})\delta(-E+K^2+2\vec{K}\cdot\vec{p}_u)\right), \tag{2}$$

where $K(E)$ is the inelastic momentum transfer $K(E)=\vec{k}-\vec{k}_n$.

Equation (2) is referred to as the first Born binary-encounter result because $-E+K^2+2\vec{K}\cdot\vec{P}=0$ represents the condition for simultaneous conservation of momentum and energy in a binary collision of two electrons. Inokuti,[11] by rewriting the argument of the δ function

$$-E+K^2+2\vec{K}\cdot\vec{p}_n=(\vec{K}+\vec{p}_n)^2-\vec{p}_n^{\,2}-E$$

gives the following elementary interpretation: The gain of the kinetic energy of the nth electron, which has momentum $\vec{P}_n$ before the collision and momentum $\vec{P}_n+\vec{K}$ after the collision, is equal to the energy E transferred from the incident particle. That is to say, the electron behaves as though it were free with a spherically symmetric momentum distribution, precisely in accordance with the neglect of the forces acting upon it within the atom. The derivation has been reproduced here in this much detail to bring out clearly the approximation leading to the binary-encounter result of Eq. (2).

B. Relation between the differential cross section and the Compton profile

The connection between Eq. (2) and Compton scattering is made when one considers the cross-section differential with respect to both solid angle and energy loss. The δ function can be written in terms of x, the cosine of the angle between $\vec{P}$ and $\vec{K}$ as $\delta(x-q/p)/2KP$, where the new variable q is defined as $(E-K^2)/2K$. Then Eq. (2) can be written

$$\frac{d^2\sigma}{dEd\Omega} = \frac{2k(E)}{kK^5(E)}\left[2\pi\int_q^\infty dp\,p\rho(p)\right] = \frac{2k(E)}{kK^5(E)}J(q), \tag{3}$$

where $J(q)$ is the Compton profile.[12] Equation (3) is valid for nonspherical targets (i.e., molecules) provided that $\rho(\vec{P})$ is replaced by the spherical average of the nonspherical $\rho(\vec{P})$.

By evaluating the interference and exchange scattering in a manner similar to that outlined above and including relativistic effects, Bonham and Tavard[9] obtain the relativistic form for the second-order differential cross section

$$\frac{d^2\sigma}{dEd\Omega} = \frac{2k(E)[1-(E/2c^2)(1-\beta)^{1/2}}{k(1-\beta^2)K(E)[K^2(E)-E^2/4c^2]^2}\cdot F_{ex}^{rel}(k,E,\theta) \times J_{BE}(q,K), \tag{4}$$

where F_{ex}^{rel} is a complicated relativistic binary-encounter exchange correction factor which can be approximated to

$$F_{ex}=1-K^2/k^2(E)+K^4/k^4(E)$$

in the nonrelativistic treatment and q is now defined by

$$q=E(1+E/4c^2)-K^2(E)/2K(E).$$

Relativistic values for k, $k(E)$, and $K(E)$ are used throughout. Note that the quantity $K^2(E)-E^2/4c^2$ is the BE relativistic energy gain for the target.

In Eq. (4) the Compton profile $J(q)$ was replaced by $J_{BE}(q,K)$, as it is the object of this work to compare[12] $J_{BE}(q,K)$ with $J(q)$ and thus establish the validity of the BE theory and also the quality of the HEEIS technique to obtain Compton profiles. The assumption that if the momentum transfer is sufficiently large, then $J_{BE}(q,K)$ becomes a function of the variable q only, i.e.,

$$\lim_{K\to\infty} J_{BE}(q,K)=J_{BE}(q) \tag{5}$$

will come under scrutiny.

The observed electron Compton profile in Eq. (4) is related to the generalized oscillator strength[11] (GOS) within the BE approximation. This relation together with Eq. (4) is used to convert the relative measured scattering intensities to relative GOS which are in turn placed on an absolute scale by the use of the Bethe sum rule.[8,11] The absolute GOS are then converted to Compton profiles within the BE theory. The normalization procedure is actually of no consequence to the determination of the Compton defect, as we will only be concerned with the shape and shift of the energy-loss profile in this work.

III. EXPERIMENT

For efficient and accurate determination of scattering cross sections, one needs (i) an electron-beam source of variable and relatively high intensity (up to 500 μa) which is stable in space and time, (ii) a high effective pumping speed (>20 000 liter/sec) vacuum system, (iii) a very precise (better than 0.002° accuracy) angular measurement system to determine the angle of electron scattering, due to the $(\sin^4\theta)^{-1}$ behavior of the Rutherford cross section, (iv) an efficient (high signal throughput) energy analyzer with high-energy resolution to eliminate the necessity of deconvoluting the data, and (v) an efficient low-noise electron-detection system.

The Steigerwald Telefocus electron gun[13] and the Faraday cup trapping the unscattered electron beam can be rotated in the scattering plane on a turntable inside a cylindrical vacuum chamber (see Figs. 1 and 2). The gas nozzle position is adjusted to coincide with the axis of rotation. The scattering angle is varied by rotating the primary beam,

as seen by the Möllenstedt electron velocity analyzer,[14] and is measured optically utilizing a calibrated, 0.001% linear scale and a $\times 200$ microscope with a 100 division reticle, as shown in Figs. 1 and 2. Upon passing through the energy-loss analyzer, the scattered electrons are detected by a solid-state silicon-wafer-type surface-barrier detector; the signal is amplified and shaped, accumulated in a multichannel analyzer, and stored on magnetic tape.

In this work the incident electron energy is between 20 and 40 keV, the angular range is 1.5°–14°, and the energy-loss spectrum is observed over a range of 0.5–5 keV, depending upon the momentum transfer and the atom or molecule being studied. The magnetic field has been reduced in the region of interest to less than 0.5 mG along the electron path by means of magnetic compensation and shielding. The electron-gun angular position is determined optically with a precision of ±0.0006°, while the angular accuracy is ±0.0015° taking magnetic fields, spatial beam stability, and alignment procedures (nozzle centering, collimating slit positioning, and zero-angle determination) into account. In lieu of discussing the important experimental design parameters in detail, some have been summarized in Table I and their effect on the Compton defect will be discussed fully in Sec. IV.

The following groups of experiments were performed:

(i) Extensive measurements of the Compton defect for helium and hydrogen at 35-keV incident energy. This completes the corroboration of the defect reported on in the previous work[7] for momentum transfers ranging from 1.3 to 12.4 a.u. (scattering angles of 1.5°–14°).

(ii) Compton defect at a constant momentum transfer of $K = 5.39$ a.u. for incident energies in the range of 20–40 keV to check the energy dependence.

(iii) Compton defect at a constant scattering angle of 8° for various incident energies in the 20–40 keV range. This is also a double check for systematic errors in angle measurement and the defect K dependence.

(iv) Compton-defect measurements at different gas target densities and incident electron beam currents (30 and 100 μA) to check for the effect of multiple scattering and deflection of the scattered electron by the unscattered beam, respectively.

(v) Compton-defect measurement for neon, molecular nitrogen, and molecular deuterium. The D_2 measurement was to ascertain whether or not the defect can be explained in terms of the recoil of the atom or molecule while the N_2 and Ne measurements would show any binding energy and/or electron correlation effects on the defect. Also, because of the p-electron character of Ne and N_2, these two systems were chosen to qualitatively test the theories discussed later in this work.

IV. RESULTS

In all cases, at least two measurements were taken by accumulating data on both sides of zero angle $\pm\theta$ and signal-averaging the results. The inelastic cross sections were converted to Compton profiles J_{BE} as discussed in Sec. II. The peak of the Compton profile was determined using the top 80% of the profile by the following method: The Compton profile was divided into 10 equal segments, the height of each segment being $\frac{1}{10}$th the height of the Compton peak. Next, the center q value (center of mass) of each segment was determined and plotted. This can be accomplished with a precision of typically ±0.002–±0.005 a.u., depending upon the momentum transfer under consideration. The profile peak center was taken to be the extrapolated q value of the top eight segments. This scheme provides a check on the symmetry of the profile and weights the q values of the upper segments more strongly.

The ideal Compton profile is symmetric in q and has its center at $q = 0$. All measured profiles were found to have their peaks shifted. It is this shift (positive or negative) of the peak from $q = 0$ that is defined to be the defect in momentum. The momentum defects quoted in this work are the momenta corresponding to the position of the measured Compton peak, where the negative sign indicates that the peak is shifted toward the elastic line, i.e., shifted in the direction of smaller energy loss.

Mention should be made of the defect uncertainties given in the tables. Table I gives experimental parameters and their corresponding effect on the defect. We shall discuss these and other parameters in two categories—random and systematic errors.

In the first category we have, among others, statistical noise. With the Compton-peak-determination scheme described above, it was possible to monitor statistical variations of the q values. These were compared with computer-generated profiles. Statistical noise obeying a Gaussian distribution was generated and superimposed on these theoretical profiles to simulate actual statistical variations. It was found that to obtain an accuracy of ±0.5 eV in the determination of the peak center, at least $5k$ counts at the Compton peak were necessary. $10k$ counts were typically accumulated, thus minimizing statistical uncertainties.

TABLE I. Experimental parameters of HEEIS.

Experimental parameters			Corresponding defect uncertainty
Electron source	type	Steigerwald telefocus gun	...
	energy	20–40 keV±10 eV	∓0.17 eV at K=6.5 a.u.
	FWHM	0.2–0.4 mm	...
	divergence	3×10^{-4} rad (0.02°)	...
	intensity	30–300 μA	no measurable effect observed
Target	type	gas jet	...
	flow rate	8.7×10^{19} molecules/sec (maximum)	+0.4 eV at K=7.2 a.u. for maximum pressure
	pressure	0.01–0.3 Torr	
	FWHM	0.5 mm	...
Energy-loss analyzer	type	Möllenstedt	...
	optimum res.	0.5 eV FWHM	...
	typical res.	1–25 eV FWHM	no measurable effect
	acceptance angle	6×10^{-3} deg	
	energy range	0–5 keV	...
	calibration accuracy	0.05–0.5 eV	0.05–0.5 eV
Angular measurement	type	optical	...
	working range	±20°	...
	accuracy	±0.0015°	±0.26 eV at K=6.5 a.u.
	precision	±0.0006°	...
Detector	type	surface barrier; silicon wafer	...
	dead time	$4.2\pm0.4\times10^{-6}$ sec	no effect
	saturation frequency	162 K	...
	noise threshold	26–30 keV at room temp.	...
		13 keV at 8 °C	...

Uncertainties in the incident electron energy and the scattering angle lead directly to shifts of the Compton profile about $q=0$. Computer-simulation experiments were performed in which both these parameters were changed, one at a time, for various momentum transfers. For $K=6.5$ a.u., for example, a ± 10-eV change in the incident energy produces a ∓ 0.17-eV shift while a $\pm 0.0015°$ change in the scattering angle yields a ± 0.26-eV shift of the profile. Several independent measurements of the high voltage established an uncertainty of ± 10 V in the 5–40-kV range. The $\pm 0.0015°$ angular accuracy includes errors due to mechanical angle calibration, residual magnetic field, gas-nozzle centering, collimating slit positioning, and zero-angle determination.

Another random error is introduced by the method of determining the peak position. With typically 10^4 counts in the Compton peak, the peak position can easily be determined to within 0.1 channel of the multichannel analyzer, from ± 0.05 to ± 0.5 eV depending upon the energy-loss range scanned by the analyzer. It should be noted that in quoting 10^4 counts in the peak, we assume that the peak is comprised of approximately 50 channels. Defect measurements performed at large scattering angles (large K) have both fewer counts in the Compton profile and fewer channels defining the peak area. This constitutes by far the greatest contribution to the defect uncertainty for measurements at large K. Experimental parameters such as electron-beam divergence, finite target size, energy-analyzer resolution, and acceptance angle do not shift the measured profile but tend to broaden it. However, the broadening due to these parameters is less than 0.01%.

As a systematic error, the effects of multiple scattering, in general a potentially serious source of error, have been discussed in detail by Barlas *et al.*[15] The effect of double scattering (after normalization) is to lower the Compton peak while making the profile asymmetric by raising the higher energy-loss side. For example, we find in a typical eight-degree spectrum that double scattering affects, without employing corrections, the Compton-peak height by less than 0.04% and produces an asymmetry of 0.36% at the full width at half-maximum (FWHM). This causes a shift of the Compton peak of 0.05% (0.4 eV) towards a larger energy loss (in the opposite direction of the Compton defect) for He, H_2, and D_2 at $\theta=8°$ (35 keV).

Another potential source of systematic error is the background contribution to the energy-loss spectrum due to electrons scattered from the gas-jet nozzle. The effect of nozzle scattering is to make the Compton profile asymmetric by raising the lower energy-loss side more than the high energy-loss side. This asymmetry could, in principle, produce a shift of the Compton peak toward the elastic line. It was found that subtraction of the nozzle scattering contribution had no measurable effect on the Compton defect (within experimental accuracy) as long as the intensity of the nozzle scattering in the valley between the elastic line and the Compton profile was less than 10% (3% was typical) of the Compton-peak intensity.

To eliminate other possible sources of systematic errors, the geometry of the energy analyzer was varied[16] and also the energy scale was directly checked by observing, at small angle, known preionization k-shell transitions of oxygen and nitrogen.[17,18] Part of the group (iv) experiments were to test for possible systematic errors resulting from an interaction between the incident electron beam and the scattered electrons. If the net effect were that the scattered electrons are repelled away from the incident beam, then the measured scattering angle would be larger than the actual scattering angle. This would lead to a negative defect since it is the measured scattering angle that is used in the analysis of the data. Experiments were performed with 30- and 100-μA electron beams and no change in the defect was found.

In summary, the defect uncertainties quoted in Tables II–V are 66% confidence error limits and are typically greater than the actual scatter of data points in Figs. 2 and 3.

The results (average defect) obtained for He, H_2, and D_2 using 35-keV incident electrons are given in Table II and Figs. 3 and 4. Included in Table II is the scattering angle, momentum transfer, and the BE Compton shift predicted for $q=0$. The He and H_2 momentum (q) defect versus the momentum transfer is plotted in Fig. 3, while the equivalent energy defect versus momentum transfer is plotted in Fig. 4. Figures 3 and 4 demonstrate the breakdown of the BE approximation with a maximum deviation of 2% of the Compton shift for He at $K=5$ a.u. and more than 4% for H_2 at $K=4$ a.u. The defect for He changes sign and becomes very large in the region of K less than 2 a.u. (1.5 a.u. for H_2). The BE theory fails catastrophically in this region as the binding energy to the target electron becomes comparable to the Compton shift. It should be noted that this occurs for He at about one and a half the K value for H_2, in good agreement with the ionization energies of the two systems. In the momentum transfer region from $K=5$ to 12.4 a.u., the defect for H_2 is less than the defect for helium and both are less than 0.5% of the Compton shift. The results for D_2 are also included in Figs. 3 and 4. No significant difference (within experi-

TABLE II. Defect measurement for 35-keV incident electrons.

θ (deg)	K (a.u.)	$E(q=0)$ [a] (eV)	Helium [b,c] Δq (a.u.)	Helium [b,c] δE (eV)	Molecular hydrogen [b,c] Δq (a.u.)	Molecular hydrogen [b,c] δE (eV)
1.5	1.3	24.6			$+0.027 \pm 0.014$ (2)	$+1.0 \pm 0.5$
2.0	1.8	44			-0.041 ± 0.005 (4)	-2.0 ± 0.2
2.5	2.3	67	$+0.007 \pm 0.009$ (2)	$+0.4 \pm 0.5$	-0.034 ± 0.004 (4)	-2.0 ± 0.2
3.0	2.7	96	-0.018 ± 0.007 (2)	-1.3 ± 0.5	-0.028 ± 0.006 (4)	-2.0 ± 0.4
3.5	3.2	130			-0.030 ± 0.003 (2)	-2.4 ± 0.2
4	3.6	176	-0.028 ± 0.003 (4)	-2.7 ± 0.3	-0.025 ± 0.003 (6)	-2.4 ± 0.3
5	4.5	273	-0.027 ± 0.004 (4)	-3.3 ± 0.5	-0.023 ± 0.002 (6)	-2.8 ± 0.2
6	5.4	394	-0.028 ± 0.003 (4)	-4.1 ± 0.4	-0.022 ± 0.002 (6)	-3.2 ± 0.3
					-0.021 ± 0.003 (2) [d]	-3.1 ± 0.4
7	6.3	520			-0.017 ± 0.002 (2)	-2.8 ± 0.3
8	7.1	681	-0.019 ± 0.003 (6)	-3.6 ± 0.6	-0.015 ± 0.003 (10)	-2.9 ± 0.6
					-0.012 ± 0.003 (2) [d]	-2.3 ± 0.6
9	8.0	857			-0.019 ± 0.004 (4)	-4.1 ± 0.9
10	8.9	1072	-0.020 ± 0.003 (6)	-4.8 ± 0.7	-0.014 ± 0.003 (4)	-3.4 ± 0.7
12	10.7	1524	-0.019 ± 0.002 (6)	-5.4 ± 0.6	-0.015 ± 0.008 (4)	-4.3 ± 2.3
14	12.4	2110	-0.016 ± 0.003 (4)	-5.4 ± 1.0	-0.012 ± 0.007 (4)	-4.1 ± 2.4

[a] Energy loss at $q=0$.
[b] Equivalent energy defect ΔE in eV, can be obtained by use of $\Delta E = [2E(q=0)/K]\Delta q$.
[c] Number of spectra taken in parentheses.
[d] Defect measurement for D_2 at 6° and 8°.

mental accuracy) was observed between D_2 and H_2. Thus the defect cannot be explained in terms of the recoil of the atom or molecule.

The results of the second and third groups of experiments performed at different incident energies are given in Tables III and IV and plotted in Figs. 5–8. Figures 5 and 6 clearly show that the Compton defect for He and H_2 is constant ($\Delta q = -0.026$ and -0.021, respectively) for a constant momentum transfer. The He and H_2 data for the constant θ (scattering-angle) experiment are in excellent agreement with the results of experiment (i) plotted as a solid line, as compared in Figs. 7 and 8. The solid line was obtained by plotting, with a simple abscissa coordinate transformation, the Δq vs K curves drawn in Fig. 3.

The Compton defects for N_2 and Ne measured at $K = 10.7$ a.u. (12° scattering angle with 35-keV incident energy) are given in Table V and were 0.2% and 0.9% of the total Compton shift, respectively. Even more interesting is the fact that the Compton defect is positive (in direction) for these two systems.

V. DISCUSSION

A. History of the Compton effect

The history of Compton scattering has been curious in the discontinuous nature of the development of this field—in particular, the experimental element of the field. Both photon and electron Compton scattering were studied in the 1930s and then essentially neglected until the late 1960s. It is interesting to note this pattern emerging again for the Compton defect. A chronology of the experimental Compton defect is given in Table VI.

Jauncey[19] showed that the distribution in energy of electrons scattered at a given angle gives directly the distribution in component velocity of the

TABLE III. Defect measurement for constant K (5.4 a.u.).

θ (deg)	E_0 (keV)	$E(q=0)$ [a] (eV)	Δq (He) [b,c] (a.u.)	Δq (H_2) [b,c] (a.u.)
5.6	40	394	-0.025 ± 0.003 (2)	-0.022 ± 0.003 (2)
6.0	35	394	-0.028 ± 0.003 (4)	-0.022 ± 0.002 (6)
6.5	30	394	-0.027 ± 0.004 (2)	-0.021 ± 0.004 (2)
8.0	20	394	-0.025 ± 0.006 (2)	-0.021 ± 0.006 (2)

[a] Energy loss at $q=0$.
[b] Equivalent energy defect ΔE in eV can be obtained by use of $\Delta E = [2E(q=0)/K]\Delta q$.
[c] Number of spectra taken in parentheses.

TABLE IV. Defect measurement for constant θ (8.0°).

K (a.u.)	E_0 (keV)	$E(q=0)$ [a] (eV)	Δq (He) [b,c] (a.u.)	Δq (H_2) [b,c] (a.u.)
7.7	40	803	-0.024 ± 0.003 (2)	-0.019 ± 0.003 (2)
7.1	35	681	-0.019 ± 0.003 (6)	-0.015 ± 0.003 (10)
6.6	30	600	-0.027 ± 0.004 (2)	-0.018 ± 0.003 (2)
5.4	20	394	-0.025 ± 0.006 (2)	-0.021 ± 0.006 (2)

[a] Energy loss at $q=0$.
[b] Equivalent energy defect ΔE in eV can be obtained by use of $\Delta E = [2E(q=0)/K]\Delta q$.
[c] Number of spectra taken in parentheses.

atomic electrons to first order in atomic-electron velocity. Hughes and Mann[20] considered the error resulting from neglecting the second-order atomic velocity term. In collaboration with Jauncey, they showed how the second-order term leads to an asymmetric profile and a slight displacement in the position of the maximum from that given by the simple theory. Using 1–4-keV incident electrons, Hughes and Mann[20] observed a positive displacement on the resultant Compton profile, but saw no consistent pattern emerge. The predicted asymmetry was too small to be detected experimentally although a 1%–2% negative displacement for x rays scattered from carbon and beryllium was observed experimentally by Ross and Kirkpatrick.[21] DuMond and Kirkpatrick[22] also observed a 1.2% negative defect for MoK$_\alpha$ x rays scattering from helium. There is certainly some doubt concerning the validity of these defect measurements, especially since subsequent experiments by Kappeler,[23] using similar experimental techniques, gave anomalous results in lithium. Ross and Kirkpatrick[24] also deduced an explicit shift formula, equivalent to Jauncey's result,[19] from relatively simple energy and momentum considerations by allowing the atom (nucleus plus remaining electrons) to recoil as the ejected electron escapes from its Coulomb field.

By applying conservation of energy and momentum for the incident electron and substituting into Ross and Kirkpatrick's[24] equations, it can be shown that the defect is proportional to $\tan^2\theta$, where θ is the scattering angle. Furthermore, if one assumes a Gaussian velocity distribution in Jauncey's second-order atomic velocity term[19] it can be shown that, by inverting the equation to given an energy distribution, the defect due to this second-order term is proportional to $\sigma^3 \tan^2\theta$, where σ is the variance of the velocity (momentum) profile and θ is the scattering angle. This result does not predict the angular dependence of the Compton defect observed in the present work (for He and H_2) and the predicted defect is an order of magnitude too large.

Bloch[25] derived a similar and more complete shift relation upon the broader basis of wave mechanical theory. Bloch showed that the interaction of the electrons with the atomic nucleus gives not only a broadening of the Compton line but also makes it asymmetric, shifting at the same time the position of the maximum intensity. The "defect of the Compton shift," as first coined by Bloch, was shown to be quadratic in the wavelength of the incident radiation. For the wavelength and observation angles used, the order of magnitude of the Compton defect given by $\delta\lambda \doteq D\lambda^2$ is of the order of magnitude of 1% of the total shift $\Delta\lambda$. Here D is a complicated constant which depends on the scattering substance and λ is the wavelength of the primary radiation. Bloch's theoretical values of D for beryllium and carbon were within 20% of the measured values of Ross

TABLE V. Defect measurement for 35-keV incident electrons.

Gas	θ (deg)	K (a.u.)	$E(q=0)$ (eV)	Δq (a.u.)	ΔE (eV)
Ne	12	10.7	1524	$+0.049 \pm 0.005$	$+14.3 \pm 1.5$
N_2	12	10.7	1524	$+0.010 \pm 0.003$	$+2.8 \pm 1.0$
N_2	10	8.9	1072	$+0.013 \pm 0.006$	$+3.3 \pm 1.5$

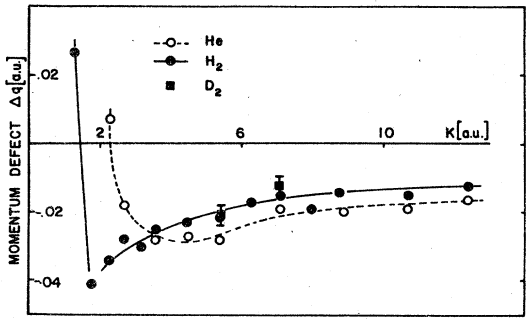

FIG. 3. Results of group (i) experiments: The momentum defect of He, H_2, and D_2. Defect values and error bars are given in Table II. $E = 35$ keV.

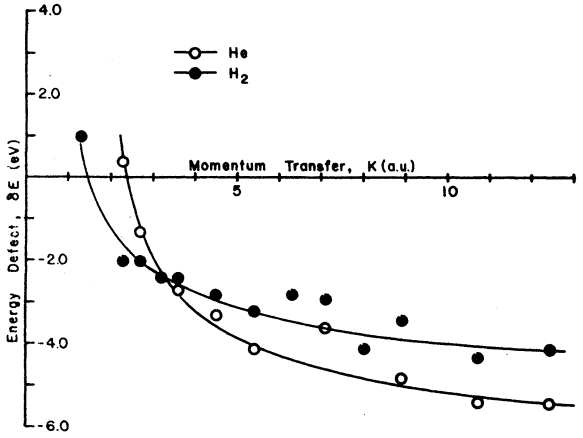

FIG. 4. Results of group (i) experiments: The energy defect of He and H_2. Defect values and error bars are given in Table II. $E = 35$ keV.

and Kirkpatrick.[21] Recently, Bloch and Mendelsohn[26] and Eisenberger and Platzman[27] have shown that the expansion Bloch[25] used in deriving his results was not a good approximation for 1s electrons and furthermore, his K and L results contain certain mathematical errors.

B. Other recent measurements of the Compton defect

x-ray measurements

Now in the 1970s, the parallel historical development of photon and electron scattering is emerging again. Weiss[28] has found for MoK_β x rays, scattered through 157.6° from an aluminum single crystal, that the center of gravity of its Compton profile was shifted about 1% (-10 ± 7 eV) towards the unmodified line. In this case it is the weakly bound valence electrons that exhibit the defect as evidenced by sharp discontinuities in the slope at the Fermi momentum. Thus Weiss suggests that it is not the binding effects of the core electrons that produce the defect, as previously thought.

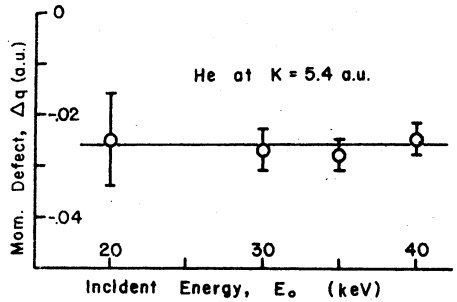

FIG. 5. Results of group (ii) experiments: The momentum defect of He measured at a constant momentum transfer of $K = 5.4$ a.u. for various incident energies. Data are from Table III. The solid line is at $q = -0.026$ a.u.

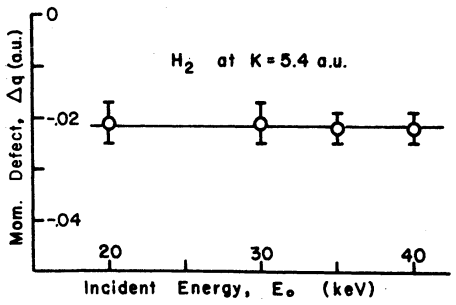

FIG. 6. Results of group (ii) experiments: The momentum defect of H_2 measured at a constant momentum-transfer of $K = 5.4$ a.u. for various incident energies. Data are from Table III. The solid line is at $q = -0.0215$ a.u.

Recently, independent Compton-defect studies using MoK_α and MoK_β x radiation were made at two laboratories by Weiss, Cooper, and Holt.[29] Polyethylene (CH_2) and lithium were chosen because the central portion of the profile is almost entirely due to valence electrons in polyethylene and because the lithium profile is so narrow that residual uncertainties in the systematic corrections to the data have a minimal effect on the location of the peak position. Weiss also made measurements on samples of both substances as well as beryllium for various target thicknesses in order to be able to eliminate the effects of multiple scattering (positive shift) which tend to cancel out any negative Compton defect. A negative 1% defect was observed in all three materials by both laboratories. From the measurements on lithium, it was found that the core and valence electron peaks occured at the same energy, suggesting that the defect is not proportional to the binding energy as given by the Ross-Kirkpatrick theory.

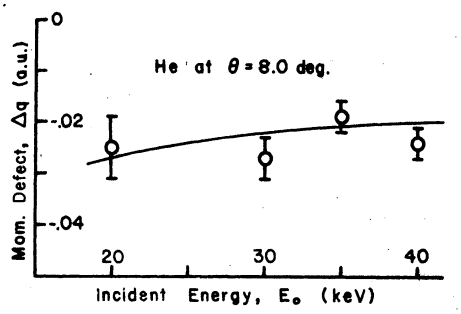

FIG. 7. Results of group (iii) experiments: The momentum defect of He measured at a constant scattering angle of $\theta = 8.0°$ for various incident energies. Data are from Table IV. The solid line is the same line as in Fig. 3 to give a comparison of the group (iii) data to the group (i) data.

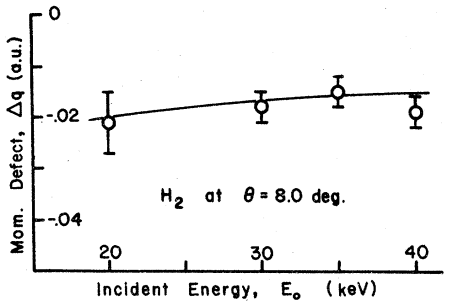

FIG. 8. Results of group (iii) experiments: The momentum defect of H_2 measured at a constant scattering angle of $\theta = 8.0°$ for various incident energies. Data are from Table IV. The solid line is the same line as in Fig. 3 to give a comparison of the group (iii) data to the group (i) data.

(e, 2e) measurement

In addition, a corresponding shift (defect) in the $(e, 2e)$ reaction involving s-state bound valence electrons of inert gas atoms has been observed by McCarthy, Noble, Ugbabe, and Weigold.[30] The $(e, 2e)$ technique is related to HEEIS by the fact that the cross section for HEEIS is the sum over all ion eigenstates of the integral of the $(e, 2e)$ cross section over the angles of the unobserved electron. McCarthy *et al.* report a +8.5 eV shift or defect of the quasifree peak in the distribution of the recoil momentum of the ion in the scattering of 200–600-eV electrons from He, +9.3 and +5.3 eV for 400- and 800-eV electrons from Ar, and +3.3 and +7.3 eV for 400- and 800-eV electrons scattered from Xe. All defect measurements are ±4 eV. That $(e, 2e)$ experiments yield a positive defect for He is not in contradiction to our results. In $(e, 2e)$ experiments, the scattered and ejected energies are identical and are half the incident energy, which is only several hundred eV. With this energy/momentum transfer, the sign of the defect is not certain. In fact, our He (and H_2) Compton defect measurement changes sign for smaller momentum transfers. McCarthy and Bonham[31] explain the defect qualitatively by use of a distorted-wave formalism. In fact, in the $(e, 2e)$ case, the problem of defect calculations has been solved by fitting Eikonal waves to elastic scattering and by carrying out rigorous but very difficult calculations using more-realistic models for the distorted waves.[32]

C. Recent theoretical contributions to the understanding of the Compton defect

At this point it may be useful to make some obvious observations. One defines the cross section for the kinematically complete BE reaction as the integral of the cross section over the direction of the momentum of the unmeasured electron—one assumes its energy is known. That is to say, in the BE approach to the scattering problem, one assumes that the incident electron transfers a large amount of energy to the atom or molecule and thus, for these collisions, the major fraction of the energy transferred then appears as the kinetic energy of the ejected electron, and the binding of the atomic electrons plays a secondary role—the Compton defect.

Traditionally, departures from the BE approximation have been discussed most often in connection with the momentum and energy transfer, each of which should be large, compared to the relevant momentum and binding energy of the atomic electron. Yet even at a momentum transfer of $K \simeq 10.7$ a.u. and energy transfer of 1 524 eV, the Compton defects are 0.4% and 0.3% for He and H_2 and 0.9% for Ne. It is also observed that for increasing values of momentum transfer, the absolute defect becomes approximately constant (0.012 and 0.017 a.u. for H_2 and He) and does not approach zero as one would expect if the BE approximation conditions have been met [see Eq. (5)]. Weiss *et al.*[29] have suggested that the Compton defect may be due to the recoil momentum transferred during the collision to the other electrons (spectator electrons) through their Coulomb repulsion. They derive a correction term and combine it with the mass of the electron (giving it a slightly larger effective mass) in the Compton-shift relation. As the same effect should be present in Compton scattering of electrons, they also show that, in the electron case, the correction term is of the order

$$(1/r_{12})[\alpha\hbar^2 c/2\pi(2mE_0^3)^{1/2}\sin 2\phi]^{1/2},$$

where E_0 is the incident electron energy and r_{12} is the distance between the ejected electron and the spectator electron. Thus the defect may be a measure of the correlation distance r_{12} and could be viewed as a many-body correction to the impulse approximation. Although the functional form of this correction term is in fair qualitative agreement with our He and H_2 data,[7] the ~20% difference (for $K = 5.4$ a.u., for example) between the He and H_2 defect is less than one would expect from the difference in r_{12} of these two systems. Moreover, in the light of our positive defect measurements for Ne and N_2, it is clear that the spectator electron model does not agree with these larger systems.

One approach in dealing with the Compton defect is to start with the cross section for a collision of two free electrons (BE approximation) and consider the binding at a succeeding step of the problem. This has been the approach in the past and

TABLE VI. Chronology of experimental Compton defect.

Year	Defect	Target substance	Probe used	Investigators
1934	−1% to 2.4%	carbon beryllium	SnK_β AgK_β scattered MoK_β at 90°	Ross and Kirkpatrick [a]
1936		lithium		Kappelar [b]
1937	−1.25%	helium	MoK_α; $\theta_{sc}=180°$	DuMond, and Kirkpatrick [c]
1938	+?	helium	1–4 keV e^-	Hughes, and Mann [d]
1968	$-\frac{1}{2}$%	beryllium	MoK_α, $\theta=120°$	Phillips, and Weiss [e]
1970	none	liquid H_2, helium	MoK_α, $\theta=134°, 170°$	Eisenberger [f]
1975	−1% (−10±7 eV)	aluminium	MoK_β, $\theta=160°$	Weiss [g]
1976	+5–10 eV ±4 eV	helium, argon, xenon	200–800 eV e^- $(e, 2e)$	McCarthy, Noble, Ugabe, and Weigold [h]
1977	−1%	polyethylene beryllium lithium	MoK_α, $\theta=160$ MoK_β $\theta=151.8$ $\theta=152.1$	Weiss, Cooper, and Holt [i]
1977	−0.2%–1% +0.9% +0.2%	helium, hydrogen neon nitrogen	20–40 keV HEEIS	Rueckner, Barlas, and Wellenstein [j]

[a] In Phys. Rev. 46, 668 (1934).
[b] In Ann. Phys. (Leipz.) 27, 129 (1936).
[c] In Phys. Rev. 52, 419 (1937).
[d] In Phys. Rev. 53, 50 (1938).
[e] In Phys. Rev. 171, 790 (1968).
[f] In Phys. Rev. A 2, 1678 (1970).
[g] In Philos. Mag. 32, 247 (1975).
[h] Private communication.
[i] In Philos. Mag. 36, 193.
[j] This paper.

has been unsuccessful since a fully detailed theory of the defect must necessarily include intricacies of the many-body problem. Moreover, it is clear from our Ne and N_2 data and the work of Weiss *et al.*[29] that the defect is not due, in any simple degree, to the binding energy. In the case of N_2 and Ne, nearly 30% of the electrons are bound by more than 400 eV, yet the defects are only 3 and 14 eV, respectively.

More recently, the approach to the problem is to explicitly include binding and a more accurate representation of the ejected electron than a plane wave in the first Born calculation. Returning to the basic equation (1), it is quite clear that more realistic final state wave functions than plane waves can be used for ψ_n. In addition, the δ function in Eq. (2) can be rewritten so that one conserves energy and momentum for the whole-system incident electron and target electron.[6] This has been carried out by Eisenberger and Platzman[30] for the hydrogenic 1*s* state and leads explicitly to a negative Compton defect.

Similarly, using an excited state of the hydrogenic potential as the final state, Bloch and Mendelsohn[26] have calculated the cross sections of bound electrons for the hydrogenic case in which the solution is "exact" within the first Born approximation. Their results for *L*-shell Compton profiles yield a negative defect for the 1*s* and 2*s* electrons, the magnitude being approximately 20% of the binding energy.

For the many-electron atom, the excited states approximation of Currat, DeCicco, and Weiss[33] and the effective hydrogenic theory of Mendelsohn and Bloch[34] yield a negative Compton defect for *s*-state electrons which decreases with increasing momentum transfer and a positive defect for *p*-state electrons which increases with increasing momentum transfer. An excellent summary discussion of the impulse approximation and the exact hydrogenic method has been given in a review by Mendelsohn and Smith.[35]

From the above we see that either positive or negative defects are possible. Because of the *p*-electron character of Ne and N_2, these two systems were chosen to qualitatively test these results. For an outer filled *p* shell, as is the case for Ne, one may expect the positive defects associated with the contribution of the six 2*p* electrons to outweigh the negative defects associated with the two 2*s* electrons. This seems to be the case in neon. The inner-shell *s* electrons will have less influence on the peak position as their profile is considerably broader. For N_2, with only three *p* electrons, one may still expect a positive defect, although considerably less than that of Ne. Again, this is the case, although to what extent these theories can be extended to molecular orbits is uncertain. For He and H_2 one would expect negative defects in agreement with our observa-

tions.

It appears that the excited-states approximation and effective hydrogenic theory are promising routes in dealing with the Compton-defect problem in HEEIS measurements while the distorted-wave formalism has been successfully employed in treating the $(e, 2e)$ defect.

Most recently, Gasser and Tavard[36] have derived a simple expression for the HEEIS Compton defect. They define a function, valid for both x rays and electron scattering, which is closely related to the generalized oscillator strength [Eq. (6)], within the first Born theory. By using the same technique Eisenberger and Platzman used in deriving the impulse approximation, they replace the energy-conserving δ-function operator by its Fourier representation, replace the exponentials by the Hamiltonian operator, and expand the Hamiltonian operator to fourth order in time. After some algebra, they cast the original function into the form of an expansion, where the first term is the impulse approximation and the defect is given by the ratio of the first derivative of the second term to the second derivative of the first term. The expression for the defect is evaluated for atomic targets by assuming (i) a spherically symmetric electron distribution and (ii) that the main contribution in the denominator arises from the field of the nucleus. Then the Compton defect becomes

$$\delta E = \frac{4z}{3\pi} \cdot \; 2\int_0^\infty dp\, x^2(p) - x(0)\int_0^\infty x(p)\, dp \;/x^2(0),$$

where $|x(\vec{p})|^2$ is the electronic density in momentum space. For the hydrogenic (ns) orbitals, Gasser and Tavard obtain δE: $1s = 2.27Z^2$ eV; $2s = 1.42Z^2$ eV; $3s = 0.76Z^2$ eV.

Unlike the spectator electron model[29] which predicts no defect for the hydrogen atom, the Bloch-Mendelsohn,[26] Currat-DeCicco-Weiss,[33] and Gasser-Tavard[36] theories yield a defect for the hydrogenic orbitals. The physical interpretation offered by Gasser and Tavard is that the defect arises from the nuclear force on the atomic electron which is suddenly accelerated in the Coulomb field of the nucleus upon impact by the incident electron. In the case of helium, one has also, in addition to the nuclear force, the contribution due to the other atomic electron (spectator electron) as given by the interaction potential. Using a simple wave function, Cappelo, Gasser, and Tavard[37] have calculated the defect for He to be

$$\delta E = 7.65 \text{ eV} \quad [\text{for } \psi = 1s(1)1s(2)].$$

Using more sophisticated wave functions, they obtain

$$\delta E = 6.08 \text{ eV (for Clementi Hartree Fock)}$$

$$\delta E = 5.18 \text{ eV} \quad [\text{for } 1s(1)1s'(2) + 1s'(1)1s(2)].$$

When they include the electron-electron interaction

$$\delta E = 6.93 \text{ eV} \quad [\text{for } 1s(1)1s(2)].$$

Thus the electron-electron interaction contributes approximately 10% to the defect, and one would expect the defect values for the more sophisticated wave functions to also be decreased by similar amounts.

To compare these theoretical results with the experimental data, it is necessary to consider the high-momentum transfer limit of the Compton defect. It is not clear from Fig. 4 whether this limit has been completely reached in the experiment, although the asymptotic behavior of the fitted curves make it possible to estimate the large K defect to be 4.4 ± 0.8 eV and 5.6 ± 0.7 eV for H_2 and He, respectively. Comparison is further complicated as Cappelo *et al.* have computed the shift of the Compton peak, whereas the experimental defects are obtained by extrapolating the center q values to the peak, as discussed earlier. The precision of this technique depends upon the exact shape of the profile near the peak, but should be within the experimental uncertainties quoted.

In spite of these problems, the agreement between this model and the experiments is encouraging in the case of He. Clearly, these calculations should be extended to the other systems measured in this work. H_2 should be of special interest because of the availability of excellent wave functions.

D. Summary and conclusions

In considering the meaning and/or consequences of the Compton defect, the approach was to attempt to quantitatively understand the accurate experimental data presented in this work within the framework of the theoretical model. As the measured intensities are converted to GOS within the first Born approximation, the question one should ask is what do we understand about the failure of the Born theory. Here, the best we can do is to state the following: A necessary but not sufficient condition for attainment of the first Born limit is to demonstrate that measurements of the GOS are independent of the incident energy. Measurements of certain moments of the GOS[15,38] in this laboratory have been shown to be independent of the incident energy and thus there is some indication that the conditions for the first Born theory are satisfied. On the other hand, we do not know the K and E dependence of the higher Born terms. But the fact that the Compton defect measurements [experiments (ii) and (iii) in this work] also are independent of the incident energy

suggests that the problem of the defect does not originate with the first Born theory itself.

We are left to conclude that the problem of the Compton defect stems from the BE approximation used to convert the GOS to Compton profiles. The problem with the BE approximation as well as the IA is obvious: The target electrons are considered to behave as though they were free with a spherically symmetric momentum distribution. Clearly, this is not the actual case, as there are forces acting on the electron within the atom during the collision. The quality of the BE approximation has also been discussed and analyzed in detail elsewhere[15] and found to be good to 1% of the peak height. Thus although the BE approximation and the IA are quite good in describing the collision process, these models break down in the high accuracy (< 1%) limit, whereas this experiment obtains better than $\frac{1}{2}$% accuracy. The Compton defect is a manifestation of this breakdown. The breakdown is actually twofold; in the lower-momentum transfer limit, the BE approximation fails catastrophically as the binding energy of the target electron becomes comparable to the Compton shift. The conditions for the validity of the BE approximation are not met in this K range. In the high-momentum transfer limit, the defect becomes approximately constant and in this region the BE approximation does not describe the intricacies of the collision process, regardless of the fact that the BE conditions have been attained.

The distorted-wave eikonal approximation of McCarthy-Weigold, the excited-states approximation of Currat-DeCicco-Weiss, and the effective-hydrogenic approximation of Mendelsohn-Bloch each deal in one way or another with the problem of the forces acting upon the ejected electron during the collision. The distorted-wave eikonal approximation has been successfully employed in quantitatively accounting for the defect in the $(e, 2e)$ reaction, while the excited states and effective hydrogenic approximations are far superior to the IA. These two latter theories have at least qualitatively accounted for the defect. That they predict a positive defect for N_2 and Ne in accordance with the measurements in this work is promising indeed.

Judgment on the Gasser-Tavard calculation for the Compton defect must be reserved until further results are given. In particular, the calculations should be extended to H_2, N_2, and Ne to show that the defect changes sign for the $2p$ electrons. Furthermore, Weiss[39] has pointed out that the expression $\delta E = \frac{1}{12} Z^2$, when applied to the carbon $1s$ electrons (Z effective $= 5\frac{11}{16}$) would yield a shift of almost 3 a.u.—a factor of almost 20 times greater than that calculated or observed by Currat *et al.*[33]

As more-accurate measurements of Compton profiles are being undertaken,[15] one is still left with the problem of defining the q scale. For the experimentalist, the easiest solution is to report the observed intensities on an energy-loss scale rather than a q scale. This leaves the theorist with the problem of comparing with experiment. Alternatively, a comparison can still be made by shifting the Compton profile by an amount equal to the defect Δq.

It is felt that the validity of the BE theory has been rigorously tested by this work and its shortcomings elucidated. It is hoped that this and continuing work in this laboratory will encourage further theoretical work on the scattering theory of comparable accuracy. In particular, it would be useful to find a simple theory to account for the Compton defect as the application of *a priori* theory to ever larger molecular systems will always require simplifying approximations.

ACKNOWLEDGMENT

This research was sponsored by the Research Corporation, under Grant No. RC7769.

[1]H. F. Wellenstein and R. A. Bonham, Phys. Rev. A 7, 1568 (1973).
[2]R. A. Bonham and H. F. Wellenstein, *Compton Scattering*, edited by B. Williams (McGraw-Hill, New York. 1977), Chap 8.
[3]H. F. Wellenstein, H. Schmoranzer, R. A. Bonham, T. C. Wong, and J. S. Lee, Rev. Sci. Instrum. 46, 92 (1975).
[4]R. Benesch, J. Phys. B 9, 2587 (1976).
[5]L. Vriens, *Case Studies in Atomic Collision Physics*, edited by E. McDaniel and M. McDowell (North-Holland, Amsterdam 1969), Chap. 6.
[6]L. Vriens, Physica (Utr.) 47, 267 (1970).
[7]A. D. Barlas, W. Rueckner, and H. F. Wellenstein, Philos. Mag. 36, 201 (1977).
[8]H. A. Bethe, Ann. Phys. (Leipz.) 5, 325 (1930).
[9]R. A. Bonham and C. Tavard, J. Chem. Phys. 59, 4691 (1973).
[10]W. Lamb, Phys. Rev. 55, 190 (1939).
[11]M. Inokuti, Rev. Mod. Phys. 43, 297 (1971).
[12]M. Cooper, Adv. Phys. 20, 453 (1971).
[13]H. Schmoranzer, H. F. Wellenstein, and R. A. Bonham,

Rev. Sci. Instrum. 46, 88 (1975).
[14]H. F. Wellenstein, J. Appl. Phys. 44, 3669 (1973).
[15]A. D. Barlas, W. H. E. Rueckner, and H. F. Wellenstein, J. Phys. B (to be published).
[16]W. H. E. Rueckner, A. D. Barlas, and H. F. Wellenstein, Rev. Sci. Instrum. 49, 76 (1978).
[17]G. R. Wight, C. E. Brion, and M. J. Van der Wiel, J. Electron Spectrosc. Relat. Phenom. 1, 457 (1972/73).
[18]M. J. Van der Wiel, Th. M. El-Sherbini, and C. E. Brion, Chem. Phys. Lett. 7, 161 (1970).
[19]G. E. M. Jauncey, Phys. Rev. 50, 326 (1936).
[20]A. C. Hughes and M. M. Mann, Phys. Rev. 53, 50 (1938).
[21]P. A. Ross and P. Kirkpatrick, Phys. Rev. 46, 668 (1934).
[22]J. W. M. DuMond and H. A. Kirkpatrick, Phys. Rev. 52, 419 (1937).
[23]H. Kappeler, Ann. Phys. (Leipz.) 27, 129 (1936).
[24]P. A. Ross and P. Kirkpatrick, Phys. Rev. 45, 223 (1934).
[25]F. Bloch, Phys. Rev. 46, 674 (1934).
[26]B. J. Bloch and L. B. Mendelsohn, Phys. Rev. A 9, 129 (1974).
[27]P. Eisenberger and P. M. Platzman, Phys. Rev. A 2, 415 (1970).
[28]R. J. Weiss, Philos. Mag. 32, 247 (1975).
[29]R. J. Weiss, M. J. Cooper, and R. S. Holt, Philos. Mag. 36, 193 (1977).
[30]I. E. McCarthy, C. J. Noble, A. Ugbabe, and E. Weigold (private communication).
[31]I. E. McCarthy and R. A. Bonham, AIP Con. Proc. 36, 255 (1976).
[32]I. E. McCarthy and E. Weigold, Phys. Rep. 27, 275 (1976).
[33]R. Currat, P. D. DeCicco, and R. J. Weiss, Phys. Rev. B 4, 4256 (1971).
[34]L. B. Mendelsohn and B. J. Bloch, Phys. Rev. A 12, 551 (1975).
[35]L. B. Mendelsohn and V. H. Smith, *Compton Scattering*, edited by B. Williams (McGraw-Hill, New York, 1977) Chap. 5.
[36]F. Gasser and C. Tavard, C. R. Acad. Sci. (to be published).
[37]C. D. Cappello, F. Gasser, and C. Tavard, C. R. Acad. Sci. (to be published).
[38]A. C. Barlas and H. F. Wellenstein (unpublished).
[39]R. J. Weiss (private communication).